Volume 1 | Number 1 | Jan 2013 | Pages 1–100

Nanoscale

www.rsc.org/nanoscale

ROYAL SOCIETY
OF CHEMISTRY

This is an *Accepted Manuscript*, which has been through the Royal Society of Chemistry peer review process and has been accepted for publication.

Accepted Manuscripts are published online shortly after acceptance, before technical editing, formatting and proof reading. Using this free service, authors can make their results available to the community, in citable form, before we publish the edited article. We will replace this *Accepted Manuscript* with the edited and formatted *Advance Article* as soon as it is available.

You can find more information about *Accepted Manuscripts* in the **Information for Authors**.

Please note that technical editing may introduce minor changes to the text and/or graphics, which may alter content. The journal's standard **Terms & Conditions** and the **Ethical guidelines** still apply. In no event shall the Royal Society of Chemistry be held responsible for any errors or omissions in this *Accepted Manuscript* or any consequences arising from the use of any information it contains.

ROYAL SOCIETY
OF CHEMISTRY

www.rsc.org/nanoscale

Real-Time Monitoring of Enzyme-Free Strand Displacement Cascade by Colorimetric Assays

Ruixue Duan,[‡] Boya Wang,[‡] Fan Hong, Tianchi Zhang, Yongmei Jia, Jiayu Huang, Abdul Hakeem, Nannan Liu, Xiaoding Lou and Fan Xia*

Key Laboratory for Large-Format Battery Materials and Systems, Ministry of Education, School of Chemistry and Chemical Engineering, Huazhong University of Science and Technology (HUST), Wuhan, China.

ABSTRACT:

Enzyme-free toehold-mediated strand displacement reaction has shown its power in building programmable DNA circuits, biosensors, molecular machines and chemical reaction networks. Here we report a simple colorimetric method using gold nanoparticles as signal generators for real-time detection of the product of strand displacement cascade. During the process, the assembled gold nanoparticles can be separated, resulting in the color change of the solution. This assay can also be applied in complex mixture, fetal bovine serum, and to detect single-base mismatch. These results suggest that this method could be of general utility to monitor more complex enzyme-free strand displacement reaction based programmable systems or further low-cost diagnostic applications.

INTRODUCTION:

Due to the stability, specificity and predictability of Watson-Crick base pairing and the programmable ability of DNA sequences, DNA hybridization plays an irreplaceable role in nanotechnology field.[1-5] Based on DNA hybridization, DNA can be served as not only the carrier of genetic information, but also the artificial designed functional devices through toehold-mediated strand displacement reaction. In this model, single-stranded DNA hybridizes with a nucleic acid duplex with an exposed single-stranded domain called toehold, which leads to the release of originally bound strand from the duplex after the branch migration process and yields a new DNA duplex with enhanced stability.

The strand displacement principle has shown its power in a number of attractive applications. First, integrated with aptamer, nucleic acids with natural ligand binding properties, strand displacement circuit can be used for amplified sensing.[6-17] For example, since the hybridization chain reactions (HCR) was reported by Pierce et al.,6 the target-activated isothermal autonomous HCR process has been used for ultrasensitive detection of target DNA[7,8] or RNA,[9] protein,[10,11] etc. Another isothermal autonomous process named catalytic hairpin assembly (CHA)[12] is also used for detection of DNA,[13] RNA,[14] adenosine,[15] etc. Second, driven by strand displacement reaction, various DNA machines are created.[18-32] For instance, DNA-based molecular switches can flip reversibly[18,19] between different conformations by external stimuli such as pH.[20-22] DNA walker can move along the DNA track by advancing the trailing

foot.[23-25] Third, at the boundary of DNA nanotechnology and computer science, mainly relying on the mechanism strand displacement reaction, artificial biomolecular reaction networks are created to exhibit dynamical behaviors and implement molecular information processing using DNA and RNA.[33-43] Soloveichik, Seelig and co-workers have reported that enzyme-free DNA based reaction network can be programmed to execute analogue temporal dynamics.[33] Also, biochemical reaction networks can be harnessed to conduct scaling up molecular computational systems reported by Qian and Winfree,[34] which is the most complex biochemical circuit ever. Among all the applications of strand displacement reaction, fluorimetry, as the most common testing method, shows its tremendous utility.

Apart from fluorimetry, gold nanoparticles (AuNPs) based colorimetry has also been widely applied[44-52] since AuNPs modified with DNA was first demonstrated by Mirkin et al. in 1996.[53] According to the powerful programmable ability of DNA, and high extinction coefficients and low cost character of AuNPs, colorimetric method is usually applied cooperated by enzymes.[54-58] For example, Gao et al. reported that ligation chain reaction can be monitored through colorimetric assay in real time.[54] Alternatively, colorimetric research for monitoring complex enzyme-free DNA-AuNP system has been rarely reported. In order to apply the colorimetric method to more complex reaction environment and monitor the dynamic process of complex system (i.e. cascaded strand displacement reactions), it is in urgent need to develop the colorimetric method.

Herein, we demonstrate a simple colorimetric method using AuNPs as signal

generators for monitoring enzyme-free strand displacement cascade in real time. As

the strand displacement cascade proceeds step by step, the product displaces the DNA

strands modified on AuNPs and makes the assembled AuNPs separate with each other,

leading the solution to turn red. The assay can also be used to detect single stranded

DNA. Therefore, DNA can be quantified or visually semi-quantified. Single-base

mismatched strand can also be distinguished by naked eyes. Moreover, even in

complex mixture, this strategy has good performances in terms of sensitivity and

specificity.

EXPERIMENTAL SECTION

Circuit preparation. After being chemically synthesized and shipped as powder,

DNA oligonucleotides are suspended in ultrapure water (Heal Force) and stored at

100 μM. C3-TAMRA strand (represent C3 strand with fluorescent group) and

C2-DABCYL strand (represent C2 strand with quencher) are annealed together at 100

nM in Tris buffer (pH 8.2) containing 25 mM Tris, 200 mM NaCl, 10% DMSO. C4

strand is added at 200 nM and C1 strand is 50 nM. The kinetics of the strand

displacement circuit is measured on the spectrofluorimeter (Agilent) by monitoring

the fluorescence with the excitation at 560 nm and the emission at 583 nm. The

sample temperature is maintained at 25 °C.

Typical procedure for DNA-Nanoparticle modification. To activate the thiol-DNA,

4 uL 1 mM DNA is mixed with 0.33 μL 500 mM HAc-NaAc buffer (pH 5.2) and 0.5

μL 10 mM TCEP. The solution is incubated for 1 h at room temperature. After that, the freshly deprotected DNA is added to 1 mL 20 nM gold nanoparticles (10 nm diameter) for 16 h incubation. Then, 10 μL 500 mM Tris-HAc buffer (pH 8.2) and 100 μL 1 M NaCl are slowly added for another 24 h incubation. To remove excess thiol-DNA, the solution is centrifuged (14000 rpm, 80 min) and the supernatant is carefully removed for three times before use. The deposited DNA-AuNPs are rinsed with 1 mL buffer containing 25 mM Tris, 100 mM NaCl, 10% DMSO, 0.005% Tween-20.

Formation of DNA-cross-linked AuNP aggregates. The two kinds of AuNPs are annealed at 1:1 molar ratio (Absorbance = 1.4) with the final concentration of NaCl 200 mM, kept at 65 °C for 10 min, and then slowly cooled to room temperature. Nanoparticles aggregate in this process.

Strand displacement cascade of AuNPs. C2 and C3 strands are annealed from 90 °C to room temperature in Tris buffer (25 mM Tris, 200 mM NaCl, 10% DMSO) at 4 μM. Then C2:C3 complex and aggregated AuNPs are mixed at equal volume to get the final concentration of C2:C3 complex 2 μM. After that, 4 μM C4 strand are added. A series of C1 at different concentrations are then added to the mixture solution and the absorbance of each sample is measured on the UV-Vis spectrometer from 800 nm to 400 nm. The sample temperature is maintained at 25 °C. All the photographs are taken after centrifuging at 4000 rpm for 10 seconds.

RESULTS AND DISCUSSION

Strategy of the assay. As shown in the Scheme, the strand displacement cascade constructing a catalytic cycle is set as the model of general strand displacement cascade. The complex C2:C3 can be triggered by C1 from the exposed toehold t*, displacing C3 strand. Afterwards, the reaction proceeds through C4 binding with the exposed toehold t* of C1:C2 complex, displacing catalyst C1 and releasing more C3 strands. In the strand displacement cascade, universal toeholds and long recognition domains for all DNA strands are used so that each strand displacement reaction in the cascade has $\triangle G \approx 0$. The product C3 strand of the strand displacement cascade is consumed by the disassembly of AuNP aggregates, which drives the reaction and shifts the equilibrium. Thus once C1 strand presents, the strand displacement cascade gets running and produces multiple C3 strand, which finally makes the solution turn red. The sequences used are listed in Supporting Information.

Optimization of the strand displacement cascade and gold nanoparticles separately. Fluorescent experiment (Figure 1) is conducted to confirm the function of the cascade. C2 and C3 are modified with quencher and fluorophore respectively. At the beginning, fluorescence is quenched due to the hybridization of C2 and C3. The intensity of fluorescence goes up along with the generation of C3.

As shown in Figure 2a, AuNPs are functioned with two different thiol modified oligonucleotide strands. One is the complementary strand of the C3 in the strand displacement cascade, the other is part of C3 strand. C3 strand can hybridize with the

strand on AuNP1 and then free AuNP2 to make AuNP aggregates disassemble. In order to circumvent the sequences on AuNPs reacting with the sequences in the cascade, the toehold and part c* on AuNP1 which have the greatest potential to bind with C2:C3 complex are 'blocked' through hybridizing with the strand on AuNP2. The AuNP aggregates can be formed by annealing these two kinds of AuNPs together. And this assembly is reversible, because the AuNP aggregates can be disassembled after DNase I digests all the DNA sequences (Figure S1).

Considering that if the surface of AuNPs is modified with too many DNA strands, because of steric effect, it will be difficult for C3 strand to get close to hybridize. Thus some short "helper" oligonucleotides (HS-TTTTA) are modified with those effective oligonucleotides at the same time to decrease the density of the effective oligonucleotides on the surface of AuNPs. Figure 2b shows that when the ratios of the effective oligonucleotides to the helper oligonucleotides are 9:1, 4:1 or 1:1, it can be observed by naked eyes that AuNPs precipitate in the bottom of the tube and the solution is colorless. While when the ratio is 1:4 or 1:9, the solution is red, indicating that AuNPs cannot fully assemble. The result of UV-absorbance is in accord with the photographs. The absorbance at 524 nm decreases when the ratio goes up. It indicates that the amount of free AuNPs decreases. When the surface of AuNPs is occupied by helper strands (i.e. 1:4 and 1:9), it will be difficult for the effective strands to hybridize with each other. Thus the less helper strands (i.e. 1:1, 4:1 and 9:1), the better assembly. On the other hand, the performance of disassembly is also highly dependent on the ratio. When the amount of effective strands greatly exceeds the helper strands

(i.e. 4:1 or 9:1), it will be difficult for AuNPs to disassemble due to steric hin-drance

and energy barrier. Figure 2c shows that when adding 100 nM C3 strand into the

solution, the values (A524/A700) of AuNPs with 1:1, 4:1 and 9:1 modification can

gradually increase, which means AuNPs can gradually disassemble. Compared with

4:1 and 9:1, the value of the solution labelled by 1:1 goes up faster. And only the 1:1

modified sample can finally turn red and be observed by naked eyes. These results

indicate that 1:1 is the best ratio for the system to function. We also demonstrate the

AuNPs modified by the effective oligonucleotides containing 4-base poly T can

aggregate better (Figure S2,S3)

Figure 3 shows the kinetics of directly adding 500 nM C3 into the AuNP

aggregates. As the single strand displacement proceeds, the value of A524/A700

increases, which represents the degree of free AuNPs. These results prove the

feasibility of the strand displacement cascade and AuNPs respectively, which lays the

foundation of our colorimetric assay.

Sensitivity and specificity of the assay. To evaluate the ability of this assay for DNA

detection, the detection limit is tested (Figure 4). When the concentration of C1

increases gradually, the value of A524/A700 rises accordingly. The threshold line is

calculated by 3σ method to evaluate the average of the control plus 3 times the

standard deviation. We achieve a detection limit of 1 nM for C1 strand according to

the principle.

Another important feature of our colorimetric system is high specificity. To verify

this, the AuNPs are firstly challenged with different strands in the strand displacement cascade (Figure 5). From the result, the AuNP aggregates cannot disassemble when mixed separately with C4, C2:C3 complex or C1. Only when C3 occurs can the solution turn red with a high value of A524/A700. It demonstrates that the AuNPs are only responsive to C3 strand and will not affect the strand displacement circuit.

Moreover, the colorimetric system can achieve naked eye detection of single-base mismatch which is the most common type of gene variation. Dating back to the first colorimetric detection of single-base mismatch put forward by Mirkin and his colleagues, the hybridization process is facilitated through heating and freezing of the solutions to differentiate imperfect targets by color change.[59] However, based on the different melting temperatures of perfect and imperfect targets, this method has the drawback of stringent temperature control, resulting in prolonging analysis time. Other AuNP-based colorimetric methods for SNP (single-nucleotide polymorphism) detection mainly focus on enzymatic reactions to improve the sensitivity or specificity.[60] Nevertheless, the expensive price and the specific recognition sequences of some enzymes may limit the application of enzyme-based colorimetric method. Here our enzyme-free method overcomes the shortcoming by saving the detection time and cost.

The mismatched sequences that can be differentiated in our method are listed in supporting information. In comparison with the mismatched sequences, only the perfect match sequence can make the solution turn red and no precipitates can be observed after centrifuging at 4000 rpm for 10 seconds. And the value of A524/A700

of each sample shows that the signal of perfect match sequence is largely higher than that of single mismatched sequences. The values of A524/A700 from mismatch bases indicate that the mismatch bases do not participate in hybridization and will not produce false mismatch signal (Figure S4).

We also test the stability of the assay. The S15 (The mismatched base is numbered as the 15th) is used as the model for single-base mismatched strand. The mixture of S15 and perfect matched strand is added into the system. Figure 6b shows that the signal keeps stable even when the concentration of the single-base mismatched strand is 200 times higher than that of perfect matched strand. These results prove that our method is specific and stable.

To show that our method has the generality for target sequence, an additional set of sequences listed in Table S2 is tested. The 2-C1 has two hang out domains (purple and green) on each side of the center hybridization domain (yellow and blue), while the C1 has only one hang out domain on the left side of the hybridization domain. Figure S5 shows that the principle of our assay can also be applied to another set of sequences. These results demonstrate the universality of the single-base mismatch discriminating effect.

Test in complex mixture. Furthermore, the performance of the colorimetric system in complex mixtures is also investigated (Figure 7a). In 1% or 10% FBS, the wavelength of absorbance peak shifts to low wavelengths, indicating AuNP aggregates have disassembled. From the photograph inserted, in 10% FBS, without adding C1, AuNPs

gather together and form precipitates in the tube. When adding C1, the solution turns red and no precipitates can be seen. It indicates that this method can be applied in FBS.

We also demonstrated the effect of complex detection environment on the limit and specificity. As showed in Figure 7b, in 10% FBS, the system can still achieve the detection limit of 1 nM C1 strand. In 10% Serum, the signal of each sample is lower than that in buffer. Without matrix effect, the reaction in buffer proceeds faster and gets equilibrium at lower concentration. Single-base mismatched strand can also be distinguished even in 10% FBS (Figure 7c). These results demonstrate that the system can perform well in 10% FBS. Neither the sensitivity nor specificity is affected in complex mixture.

CONCLUSIONS

In conclusion, we firstly use the colorimetric method to real-time monitor the process of strand displacement cascade. This strategy also shows the feasibility for DNA detection with a detection limit of 1 nM. More importantly, this assay exhibits a strong specificity for SNP detection. Multiple SNPs from different bases of DNA target can be discriminated very well. The specificity and stability are also attractive in complex mixtures. We believe such a real-time colorimetric method may also lead to the development of a simple and portable system of point-of-care.

AUTHOR INFORMATION

Corresponding Author

xiafan@hust.edu.cn

Author Contributions

†These authors contributed equally. The authors declare no competing financial interests.

Supporting Information

Experimental procedures and analytical data are provided. This material is available free of charge via the Internet at http://pubs.rsc.org.

REFERENCES

(1) N. C. Seeman, *Annu. Rev. Bioph. Biom.,* 1998, **27**, 225-248.

(2) J. J. Storhoff and C. A. Mirkin, *Chem. Rev.*, 1999, **99**, 1849-1862.

(3) M. M. C. Cheng, G. Cuda, Y. L. Bunimovich, M. Gaspari, J. R. Heath, H. D. Hill, C. A. Mirkin, A. J. Nijdam, R. Terracciano, T. Thundat and M. Ferrari, *Curr. Opin. Chem. Biol.,* 2006, **10**, 11-19.

(4) N. C. Seeman, *Nature*, 2003, **421**, 427-431.

(5) N. C. Seeman, *Trends. Biochem .Sci.*, 2005, **30**, 119-125.

(6) R. M. Dirks and N. A. Pierce, *Proc. Natl. Acad. Sci. USA*, 2004, **101**, 15275-15278.

(7) J. Huang, Y. R. Wu, Y. Chen, Z. Zhu, X. H. Yang, C. J. Yang, K. M. Wang and W. H. Tan, *Angew. Chem. Int. Ed.,* 2011, **50**, 401-404.

(8) Y. Chen, J. Xu, J. Su, Y. Xiang, R. Yuan and Y. Q. Chai, *Anal. Chem.,* 2012, **84**, 7750-7755.

(9) H. M. T. Choi, J. Y. Chang, L. A. Trinh, J. E. Padilla, S. E. Fraser and N. A. Pierce, *Nature biotechnology,* 2010, **28**, 1208-U1103.

(10) W. Q. Song, K. L. Zhu, Z. J. Cao, C. W. Lau and J. Z. Lu, *Analyst,* 2012, **137**, 1396-1401.

(11) B. Zhang, B. Q. Liu, D. P. Tang, R. Niessner, G. N. Chen and D. Knopp, *Anal.*

Chem., 2012, **84**, 5392-5399.

(12) P. Yin, H. M. T. Choi, C. R. Calvert and N. A. Pierce, *Nature*, 2008, **451**, 318-U314.

(13) A. X. Zheng, J. Li, J. R. Wang, X. R. Song, G. N. Chen and H. H. Yang, *Chem. Commun.*, 2012, **48**, 3112-3114.

(14) B. L. Li, A. D. Ellington and X. Chen, *Nucleic Acids Res.,* 2011, **39**.

(15) B. Fu, J. C. Cao, W. Jiang and L. Wang, *Biosens. Bioelectron.*, 2013, **44**, 52-56.

(16) F. Wang, C. H. Lu and I. Willner, *Chem. Rev.*, 2014, **114**, 2881-2941.

(17) D. Y. Zhang, A. J. Turberfield, B. Yurke and E. Winfree, *Science*, 2007, **318**, 1121-1125.

(18) Z. G. Wang, J. Elbaz, F. Remacle, R. D. Levine and I. Willner, *Proc. Natl. Acad. Sci. USA*, 2010, **107**, 21996-22001.

(19) C. Zhou, Z. Q. Yang and D. S. Liu, *J. Am. Chem. Soc.*, 2012, **134**, 1416-1418.

(20) S. Surana, J. M. Bhat, S. P. Koushika and Y. Krishnan, *Nat Commun*, 2011, **2**.

(21) S. Modi, M. G. Swetha, D. Goswami, G. D. Gupta, S. Mayor and Y. Krishnan, *Nature Nanotech.*, 2009, **4**, 325-330.

(22) J. Elbaz, Z. G. Wang, R. Orbach and I. Willner, *Nano Lett.*, 2009, **9**, 4510-4514.

(23) J. S. Shin and N. A. Pierce, *J. Am. Chem. Soc.,* 2004, **126**, 10834-10835.

(24) K. Lund, A. J. Manzo, N. Dabby, N. Michelotti, A. Johnson-Buck, J. Nangreave, S. Taylor, R. J. Pei, M. N. Stojanovic, N. G. Walter, E. Winfree and H. Yan, *Nature,* 2010, **465**, 206-210.

(25) P. Yin, H. Yan, X. G. Daniell, A. J. Turberfield and J. H. Reif, *Angew. Chem. Int. Ed.*, 2004, **43**, 4906-4911.

(26) J. Bath and A. J. Turberfield, *Nature Nanotech.*, 2007, **2**, 275-284.

(27) T. Omabegho, R. Sha and N. C. Seeman, *Science*, 2009, **324**, 67-71.

(28) Z. G. Wang, J. Elbaz and I. Willner, *Angew. Chem. Int. Ed.*, 2012, **51**, 4322-4326.

(29) M. H. Liu, J. L. Fu, C. Hejesen, Y. H. Yang, N. W. Woodbury, K. Gothelf, Y. Liu and H. Yan, *Nat Commun.*, 2013, **4**.

(30) D. Y. Zhang and G. Seelig, *Nat. Chem.*, 2011, **3**, 103-113.

(31) R. A. Muscat, J. Bath and A. J. Turberfield, *Nano Lett.*, 2011, **11**, 982-987.

(32) S. F. J. Wickham, J. Bath, Y. Katsuda, M. Endo, K. Hidaka, H. Sugiyama and A. J. Turberfield, *Nature Nanotech.*, 2012, **7**, 169-173.

(33) Y. J. Chen, N. Dalchau, N. Srinivas, A. Phillips, L. Cardelli, D. Soloveichik and G. Seelig, *Nature Nanotech.*, 2013, **8**, 755-762.

(34) L. Qian and E. Winfree, *Science*, 2011, **332**, 1196-1201.

(35) F. C. Simmel, *Acs Nano*, 2013, **7**, 6-10.

(36) A. Padirac, T. Fujii and Y. Rondelez, *Proc. Natl. Acad. Sci. USA*, 2012, **109**, E3212-E3220.

(37) G. Seelig, D. Soloveichik, D. Y. Zhang and E. Winfree, *Science*, 2006, **314**, 1585-1588.

(38) E. Franco, E. Friedrichs, J. Kim, R. Jungmann, R. Murray, E. Winfree and F. C. Simmel, *Proc. Natl. Acad. Sci. USA,* 2011, **108**, E784-E793.

(39) T. Fujii and Y. Rondelez, *Acs Nano*, 2013, **7**, 27-34.

(40) J. Kim, K. S. White and E. Winfree, *Mol. Syst. Biol.*, 2006, **2**.

(41) J. Kim and E. Winfree, *Mol. Syst. Biol.*, 2011, **7**.

(42) A. Padirac, T. Fujii, A. Estevez-Torres and Y. Rondelez, *J. Am. Chem. Soc.,* 2013, **135**, 14586-14592.

(43) C. C. Santini, J. Bath, A. J. Turberfield and A. M. Tyrrell, *Int. J. Mol. Sci.*, 2012, **13**, 5125-5137.

(44) K. Saha, S. S. Agasti, C. Kim, X. N. Li and V. M. Rotello, *Chem. Rev.*, 2012, **112**, 2739-2779.

(45) R. Elghanian, J. J. Storhoff, R. C. Mucic, R. L. Letsinger and C. A. Mirkin, *Science*, 1997, **277**, 1078-1081.

(46) T. A. Taton, C. A. Mirkin and R. L. Letsinger, *Science*, 2000, **289**, 1757-1760.

(47) D. G. Georganopoulou, L. Chang, J. M. Nam, C. S. Thaxton, E. J. Mufson, W. L.

Klein and C. A. Mirkin, *Proc. Natl. Acad. Sci. USA*, 2005, **102**, 2273-2276.

(48) D. A. Giljohann, D. S. Seferos, P. C. Patel, J. E. Millstone, N. L. Rosi and C. A. Mirkin, *Nano Lett.*, 2007, **7**, 3818-3821.

(49) J. S. Lee, M. S. Han and C. A. Mirkin, *Angew. Chem. Int. Ed.*, 2007, **46**, 4093-4096.

(50) J. S. Lee, P. A. Ulmann, M. S. Han and C. A. Mirkin, *Nano Lett.*, 2008, **8**, 529-533.

(51) D. S. Seferos, A. E. Prigodich, D. A. Giljohann, P. C. Patel and C. A. Mirkin, *Nano Lett.,* 2009, **9**, 308-311.

(52) K. Zhang, L. L. Hao, S. J. Hurst and C. A. Mirkin, *J. Am. Chem. Soc.,* 2012, **134**, 16488-16491.

(53) C. A. Mirkin, R. L. Letsinger, R. C. Mucic and J. J. Storhoff, *Nature*, 1996, **382**, 607-609.

(54) W. Shen, H. M. Deng and Z. Q. Gao, *J. Am. Chem. Soc.,* 2012, **134**, 14678-14681.

(55) W. Xu, X. J. Xue, T. H. Li, H. Q. Zeng and X. G. Liu, *Angew. Chem. Int. Ed.*, 2009, **48**, 6849-6852.

(56) H. X. Li and L. J. Rothberg, *J. Am. Chem. Soc.,* 2004, **126**, 10958-10961.

(57) J. H. Li, X. Chu, Y. L. Liu, J. H. Jiang, Z. M. He, Z. W. Zhang, G. L. Shen and R.

Q. Yu, *Nucleic Acids Res.,* 2005, **33**.

(58) W. Wu, J. H. Chen, Z. Y. Fang, C. C. Ge, Z. C. Xiang, C. Y. Ouyang, P. C. Lie, Z. Xiao, L. X. Yu, L. Wang and L. W. Zeng, *Anal Chim Acta*, 2013, **804**, 235-239.

(59) R. Elghanian, J. J. Storhoff, R. C. Mucic, R. L. Letsinger and C. A. Mirkin, *Science*, 1997, **277**, 1078.

(60) H. X. Li and L. J. Rothberg, *J. Am. Chem. Soc.*, 2004, **126**, 10958.

Figure caption

Scheme. This figure represents the colorimetric method for monitoring enzyme-free strand displacement cascade. The product of the catalytic strand displacement cascade, C3 strand, is consumed by disassembly of AuNP aggregates.

Figure 1. The strand displacement cascade can be triggered by C1 from the exposed toehold t* of complex C2:C3 with fluorescence quenched, displacing C3 strand and producing fluorescence signal. Afterwards, the reaction proceeds through C4 binding with the exposed toehold t* of C1:C2 complex, followed by displacing catalyst C1, which helps to free more C3 strands. The progress is monitored through fluorescence signal. The concentration of C2:C3 is 100 nM. C4 is 200 nM. C1 is 50 nM.

Figure 2. (a) The disassembly of aggregated AuNPs. (b) The effect of ratio between the effective oligonucleotides and the helper oligonucleotides on making AuNPs aggregate and corresponding photographs. Only when the ratio is above 1:1, the AuNP aggregates can be clearly seen after annealing. (c) The effect of the ratio between the effective oligonucleotides and the helper oligonucleotides on making aggregated AuNPs disassemble, and corresponding photographs: when the ratio is 1:1, aggregated gold nanoparticles can easily disassemble.

Figure 3. Time-dependent value changes of A524/A700 after 500 nM C3 added is shown.

Figure 4. Investigation of the sensitivity. To lower the leak reaction, the concentration of each strand is half of that in kinetic experiment. The concentration of C2:C3 is 1 μM. C4 is 2 μM.

Figure 5. The aggregated AuNPs is highly selective to react with C3 and resist C4, the concentration of C2:C3 and C1 is500 nM, respectively.

Figure 6. (a) Investigation of single-base mismatch detection. The concentrations of mismatched strand and perfect match strand (PM) are 500 nM. The bar graph shows the value of A524/A700 of each single-base mismatched sample and perfect match sample. The corresponding photograph shows that only the perfect match sequence can make the solution turn red and no precipitates can be observed after centrifuging at 4000 rpm for 10 seconds. (b) Effects of varying amounts of single-base mismatched strand mixing with perfect matched strand.

Figure 7. (a) UV-vis spectra of the colorimetric system performed in FBS and photographs taken for 10% FBS samples are shown. (b) Investigation of the sensitivity in 10% FBS and buffer. The con-centration of C2:C3 is 2 μM. C4 is 4 μM. (c) Investigation of the specificity in 10% FBS. The concentrations of mismatched strand and PM are 100 nM. The bar graph shows the value of A524/A700 of each single-base mismatched sample and perfect match sample.
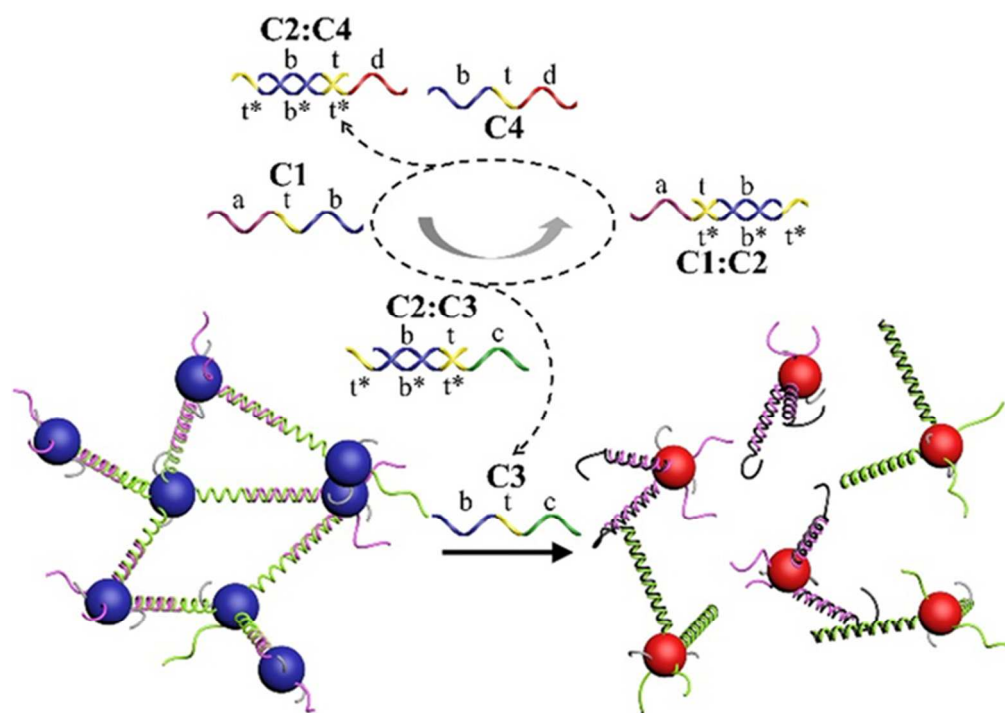
60x42mm (300 x 300 DPI)
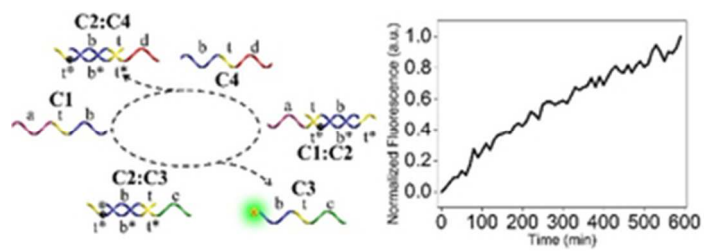
29x10mm (300 x 300 DPI)
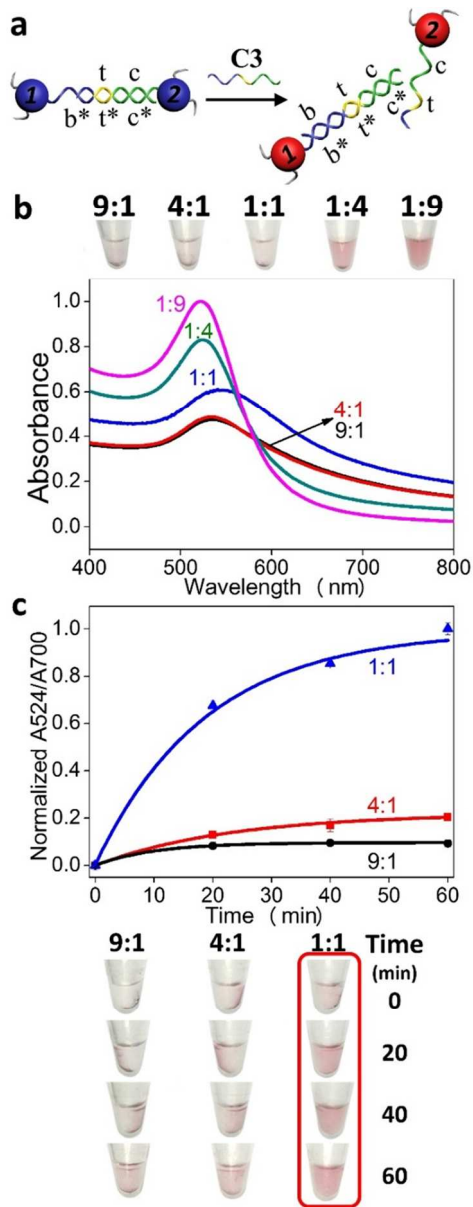
216x555mm (300 x 300 DPI)
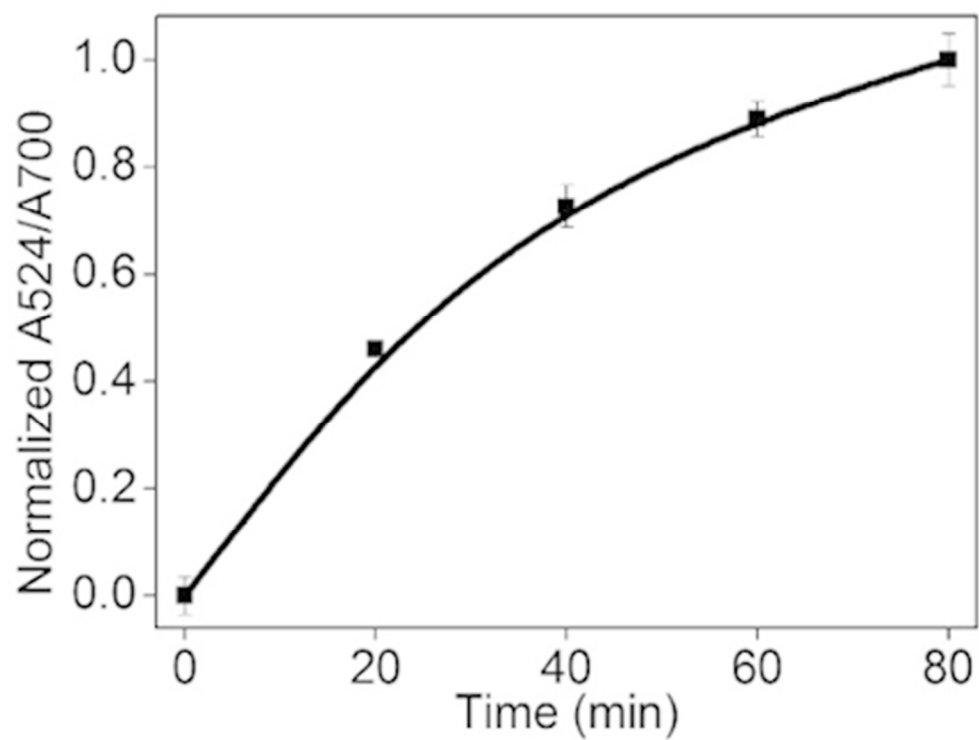
63x47mm (300 x 300 DPI)
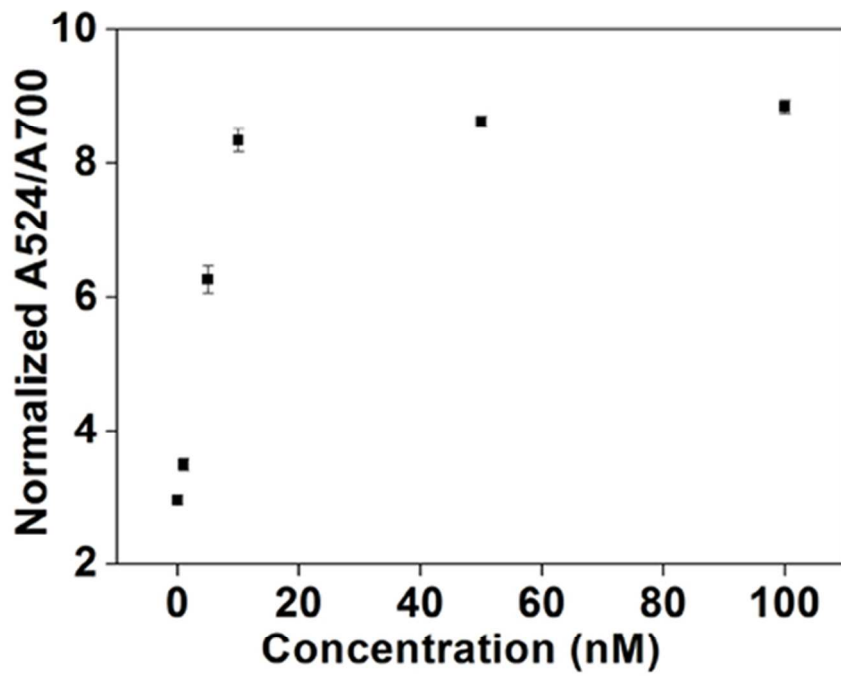
68x56mm (300 x 300 DPI)
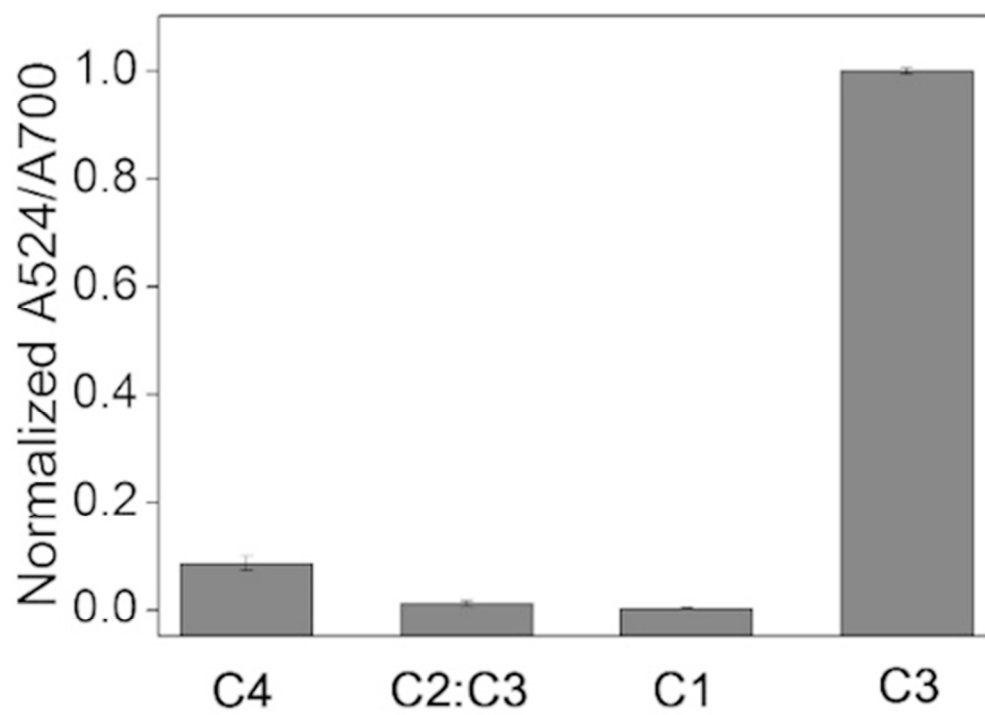
61x44mm (300 x 300 DPI)
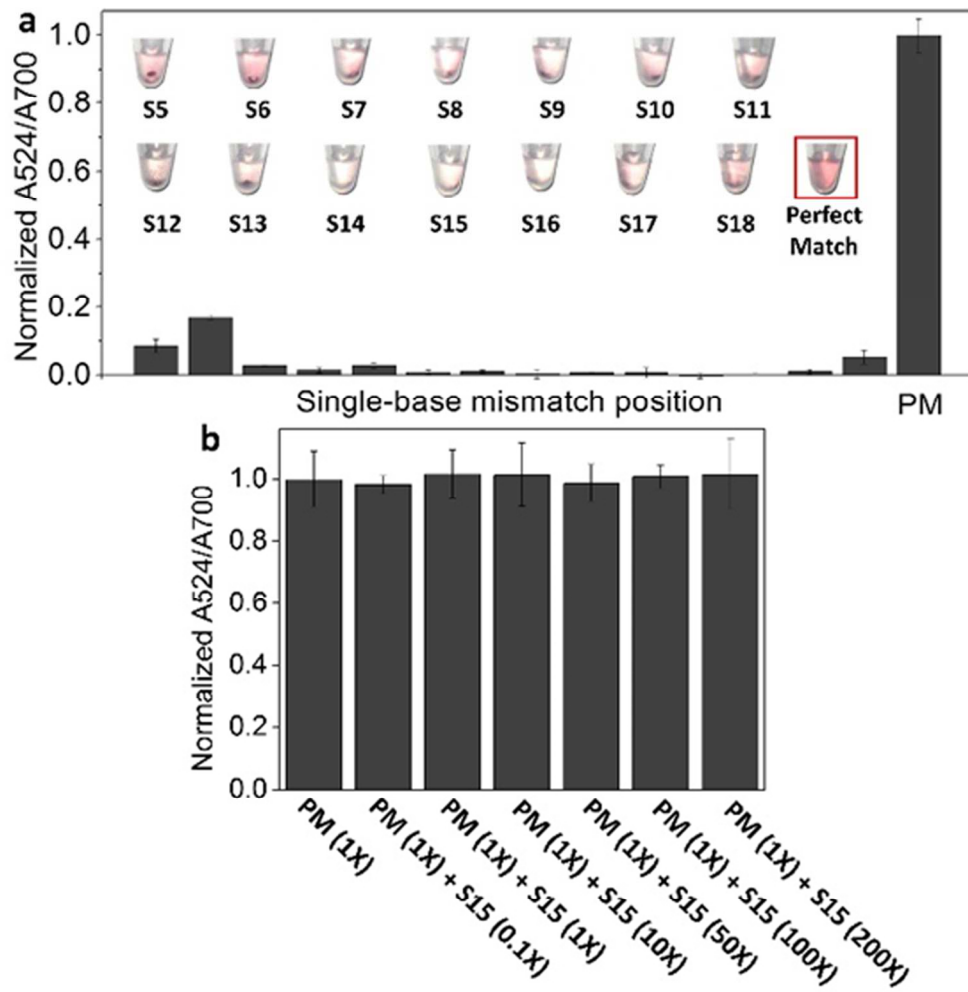
84x84mm (300 x 300 DPI)

156x290mm (300 x 300 DPI)